Advanced System Design and Control Aspects in a Fuel-Optimal Hybrid Vehicle

E. Shafai, Ph. Dietrich, Ch. Wittmer, and S. Ginsburg

Department of Mechanical Engineering
Swiss Federal Institute of Technology (ETH) Zurich, Switzerland
shafai@imrt.mavt.ethz.ch, dietrich@lvv.iet.mavt.ethz.ch

Abstract

Electric vehicles today clearly represent the only solution fulfilling the zero emission vehicles (ZEV) standard. However, they still are not an equivalent alternative to the gasoline driven cars due to the well known problems of today's batteries. The concept of a parallel hybrid drive line can be an optimal combination of both principles of propulsion in that the gasoline engine guarantees for a wide range operation, while the electric propulsion can be used within the restricted zero emission zones.

The parallel hybrid solution described here has been realized in the "Hybrid III" research and development project at the Swiss Federal Institute of Technology (ETH), Zurich, Switzerland. The drive line consists of a gasoline engine, an electric asynchronous motor/generator, a flywheel, and a wide range continuously variable transmission. It is shown how these components cooperate in a fuel-optimal way. This drive line is now about to be integrated in a vehicle for real road testing. This paper describes the control aspects of this complex hybrid vehicle and introduces the experimental results on a dynamic test bench verifying its operation under realistic traffic conditions.

1 Introduction

The concept of the innovative drive line developed in the "Hybrid III" research project (depicted in Figure 1) has been reported in detail in a number of publications ([6], [12], [14], and [16]). However, for the sake of completeness, it is summarized in this section.

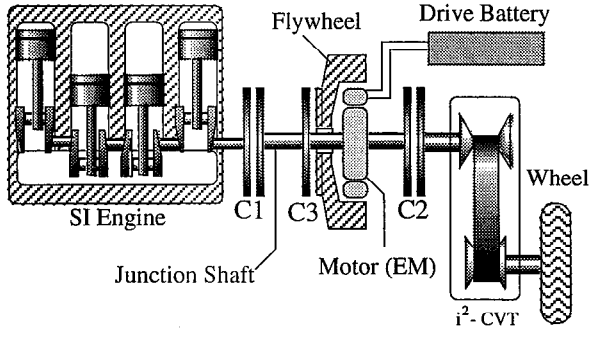

Figure 1: ETH Hybrid III drive line.

This parallel hybrid drive line combines a gasoline engine (1.3 l VW, 53 kW), an electric asynchronous motor (6 kW) / generator (16 kW), a fairly small set of Ni-MH batteries (5 kWh), a flywheel (1.24 kgm^2) for storing up to 0.068 kWh of mechanical energy at 100 Hz, (corresponding to the vehicle's braking energy from 70 km/h down to standstill), and a wide range i^2-CVT with the expanded range of 20.5:1.

The three dry clutches C1, C2, and C3 are used to operate the Hybrid III drive line in the following four configurations:

SI engine connected directly to the CVT. The SI engine and the continuously variable transmission are directly coupled by the closed clutches C1 and C2. The flywheel is disengaged, while clutch C3 is open. This is the conventional configuration of a car with a CVT, except that here the output torque can be boosted by additionally using the electric motor (EM).

SI engine combined with flywheel. In this configuration the clutches C2 and C3 remain closed. The flywheel is responsible for delivering the power requested by the drive line. Once the flywheel is discharged, it is reloaded by the SI engine.

EM connected directly to the CVT. This is the conventional configuration of a zero emission vehicle. Power is delivered to the wheels by the electric motor and the CVT, while clutches C1 and C3 are opened (SI engine and flywheel both are disengaged) and C2 is closed. The acceleration capabilities are limited by the power rating (6 kW) of the electric motor. However, this power level is certainly too low to be attractive to a typical driver.

EM combined with the flywheel. This is yet another configuration of a zero emission vehicle. Power is delivered to the wheels by the electric motor and, if necessary, by the decelerating flywheel. The speed of the flywheel is maintained at a sufficiently high level by using the excess of the power delivered by the electrical machine over the average power demand of the wheels and by mechanical regenerative braking. Furthermore, electric regenerative braking helps to prevent the premature exhaustion of the drive batteries.

A fuel optimal operating strategy based on these possible configurations is developed for the hybrid vehicle to operate in real road traffic. This operating strategy is described in detail in [6] and [12]. It is summarized in the next section of this paper. The brief introduction of the most important control problems posed by the realization of this operating strategy and the experimental results showing the dynamic behaviour of the controller implemented are the main subjects of this paper.

The development and the control aspects of the electrical machine, however, would exceed the scope of this paper. They are described in detail in [7] and [8].

Aside from the fuel optimality and emission aspects, another important issue is the drivability of the hybrid vehicle. It has been investigated in [3] theoretically, based on a simple model of the Hybrid III drive line. The experimental results presented in this paper confirm the simulation results introduced in [3].

2 Operating Strategies

In order to achieve the highest possible efficiency, a sophisticated operating strategy is mandatory. We distinguish the three following principal operating strategies:

- FBOS: Fuel Based Operating Strategy
- EBOS: Electricity Based Operating Strategy
- FBEBOS: Combination of FBOS and EBOS

The focus of this paper is on the first operating strategy (FBOS). The latter two are described in [12].

To achieve the highest possible efficiency in FBOS, depending on the power requested by the driver, one of the following operating modes is selected:

Duty cycle operating mode. For low power demand (< 12 kW), the drive line is configured as an *"SI engine combined with flywheel,"* as described in the previous section. When the speed of the flywheel drops below a certain limit (i.e., flywheel discharged), clutch C1 is closed, the combustion engine starts, and it runs at full load with a high fuel efficiency to accelerate the flywheel. When the speed of the flywheel reaches an upper limit, clutch C1 is opened and the combustion engine is stopped.

The efficiency potential of the duty cycle mode in comparison to variable inlet valve timing is described in [4] and [5]. The upper and lower limits of the flywheel speed (3600 rpm and 1800 rpm, respectively) for stopping and starting the engine are found by an efficiency optimization as described in [6].

Highway operating mode. For high power demand (> 14 kW), the drive line is configured as an *"SI engine connected directly to the CVT."* In this mode the engine runs at full load with a high fuel efficiency while the CVT controls the power requested by the driver.

Throttle operating mode. The drive line configuration is the same as in the highway mode. This mode is selected when the power demand is within the power range in-between duty cycle mode and highway mode (12 KW-14 kW). That range as well was found by an optimization process as described in [6]. In this mode the power requested is controlled by throttling the engine, while the engine is operating at minimum speed (controlled by the CVT).

The principal strategy for changing from duty cycle mode either into the highway mode or into the throttling mode is to totally discharge the flywheel before starting the engine. The decision for a change is therefore made at the lower speed limit of the flywheel.

Regenerative braking. The flywheel is a highly efficient device for storing energy. The braking energy is recuperated therefore by the flywheel as the first priority. Once the flywheel is fully charged at 100 Hz, the braking energy is converted into electric energy (i.e., the battery is loaded) by operating the electric machine as generator. The efficiency of storing energy in a battery is rather low at high current levels. Therefore, battery storage is used as a second priority only. The lowest priority is given to the use of the braking energy for heating up the oil in the gear box and in the engine. This reduces the friction losses after long engine shut-down periods.

The results obtained on a dynamic powertrain test bench are given in Table 1. They demonstrate the efficiency of the Hybrid III drive line with the operating strategies introduced in this section. Please note that for the Hybrid III vehicle a test mass of 1500 kg was assumed. The difference to the mass of the standard 1.6 l VW Golf III is due to the additional weights of the battery and of the Hybrid III drive line.

Test Cycle	Hybrid III	Reference
ECE-R15/04	4.7	8.9 a)
FTP75	5.0	-
ICC-Zurich *)	5.9	10.9 b)

Table 1: Efficiency of the ETH Hybrid III powertrain compared to the reference car:

a) VW Golf III, 1.6 l, 55 kW, mass of the empty car 1015 kg,
b) VW Golf III, 1.3 l, 44 kW, test mass 1135 kg.
*) ICC-Zurich is the inner city cycle for Zurich. It is a typical cycle for urban driving in Zurich, synthesised by measurements.

3 Control Aspects

Sections 3.1 through 3.6 briefly introduce the most important control problems encountered in the Hybrid III project.

3.1 Control of the Hydraulic Power Supply

The scheme of the hydraulic power supply is shown in Figure 2. The power supply has three different pressure levels. The pressure in the hydraulic storage volume is the highest at $p_H \approx 80$ bar. It is used for actuating the clutches. A simple relay controller with a hysteresis band from 50 to 80 bar is used to control the pressure in the hydraulic storage volume by actuating the valve V_1.

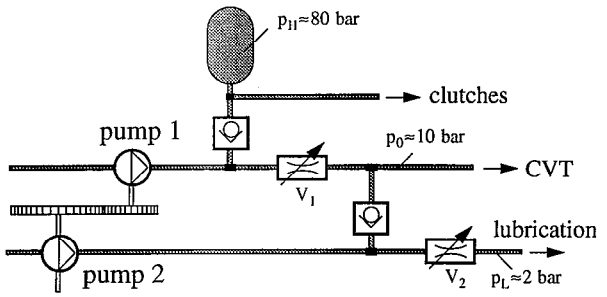

Figure 2: Scheme of the hydraulic power supply

The next lower pressure level ($p_0 \approx 10$ bar) is used for changing the transmission ratio of the CVT. A large drop of the pressure below 10 bar could cause damage to the CVT's belt and is therefore to be avoided.

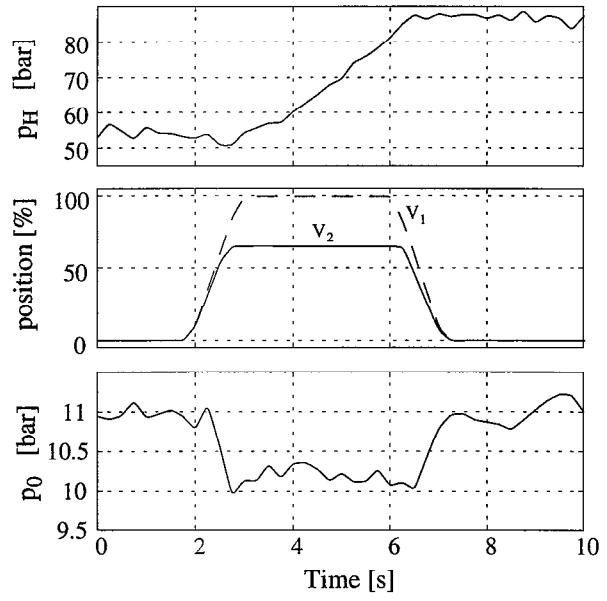

Figure 3: Loading of the hydraulic storage volume

To prevent the pressure from dropping too low, the valve V_2 is controlled in function of the position of the valve V_1, the speed of the shaft driving the pumps, and the desired rate of change of the CVT's gear ratio. The result of this control strategy during a loading process of the hydraulic storage volume is shown in Figure 3. It clearly shows that the drop of the pressure is kept small even during this loading process.

The lowest pressure level ($p_L \approx 2$ bar) is used for lubrication and cooling the CVT's belt. This pressure level has the lowest importance in the control strategy.

3.2 Control of the Dry Clutches

For the control of the dry clutches, the pressure in their hydraulic actuating cylinder (servo motor) is controlled. The control scheme is shown in Figure 4.

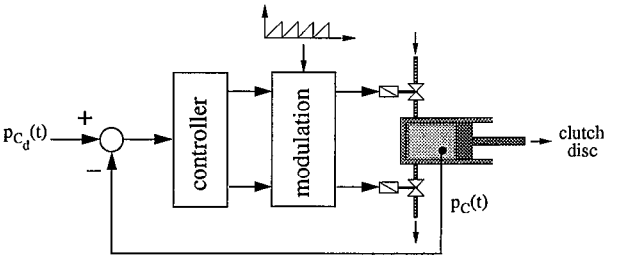

Figure 4: Scheme of the clutch pressure control

For the clutch pressure control, highly sealing solenoid valves (input and output valves) are used. Their high sealing quality allows to realize a totally opened or closed clutch without the oil flow having to be throttled. This capability increases the total efficiency of the drive line.

The actuating signals for the valves are generated by modulation of the control signals with a sawtooth signal. The frequency of the sawtooth signal (300 Hz) is much higher than the highest switching frequency of the valves. This causes the valve body to beat in a middle position for a medium control signal. If the control signal is higher than the amplitude of the sawtooth signal, saturation occurs and the valve opens completely.

For a negative control error, the controller acts as a PID controller for the input valve and generates a negative signal for the output valve in order to close it completely, and vice versa in the case of a positive control error.

3.3 Realization of the i^2-CVT

The realization of the i^2-CVT is shown in Figure 5. A total of four jaw clutches are used. In the low gear, two of them (jc 1a and jc 2b) are engaged while the transmission ratio is changed from $i = 0.42$ to the synchronizing ratio of $i_S = 1.93$. As shown in Figure 6, this range corresponds to a total transmission ratio of $\nu = 46.2$ to $\nu_S = 10$.

For shifting into the high gear, input and output shafts of the CVT are reversed by opening the jaw clutches jc 1a and jc 2b, while closing jc 2a and jc 1b. Before closing a jaw clutch, two things are checked: the corresponding opening jaw clutch must be open and the relative speed over the closing jaw clutch may not be above 50 rpm.

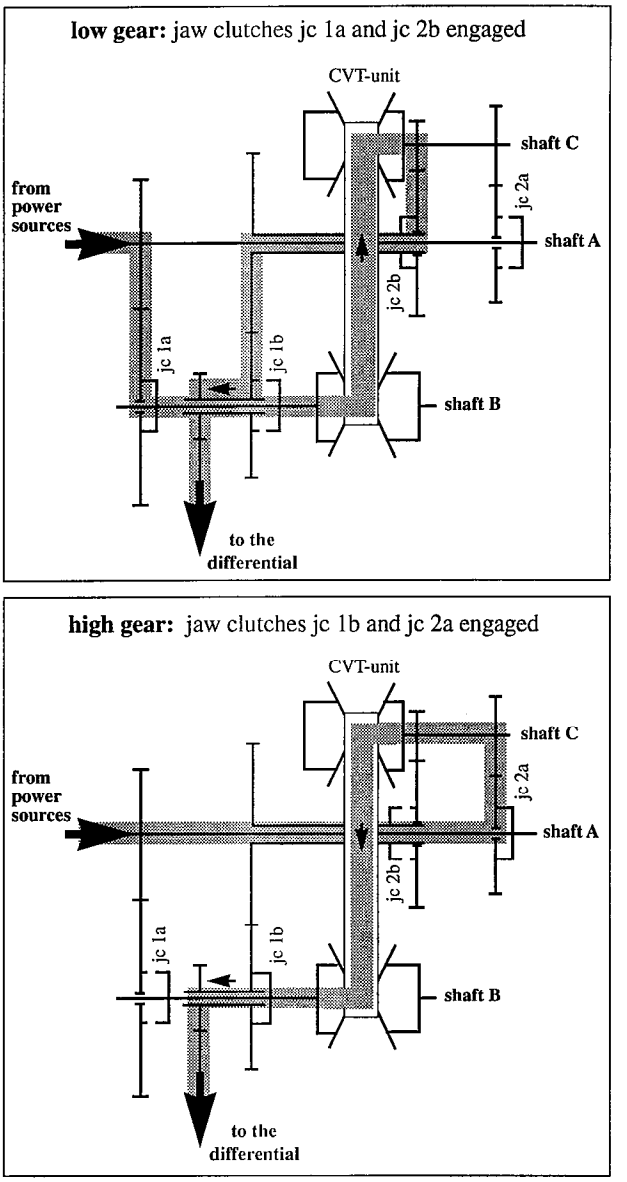

Figure 5: Power flow through the i^2-CVT

In high gear, the transmission ratio of the CVT can be changed back from the synchronizing ratio to the ratio of $i = 0.42$, which corresponds to a total transmission ratio of $\nu = 2.2$ (see Figure 6).

For the jaw clutch control highly sealing solenoid valves similar to those mentioned in section 3.2 are used. The average duration for engaging a jaw clutch is 150 ms, or 100 ms for disengaging, respectively. Consequently, the time required for a shift between low and high gear, including a sequence of two opening and two closing jaw clutches, is about 500 ms.

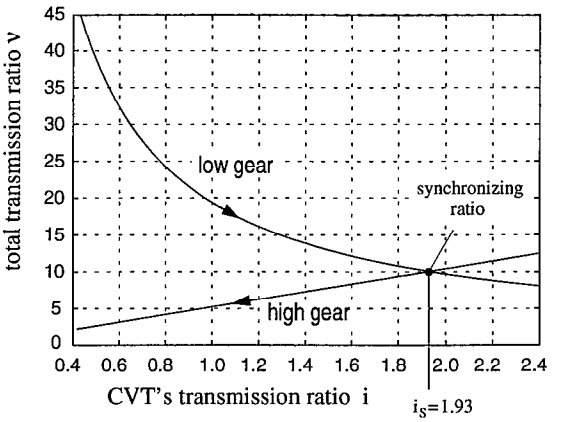

Figure 6: Relation between total transmission ratio and CVT's transmission ratio

The effect of these gear shifts on the drivability of the Hybrid III vehicle is shown in Figure 7. This sequence includes a regenerative braking and the subsequent acceleration of the vehicle. The top and the middle graph also clearly show the efficiency of the recuperation. The braking energy gained by braking the vehicle from 70 km/h to a standstill is capable to fully load the flywheel which then accelerates the vehicle from zero to about 50 km/h. This corresponds to a recuperation efficiency of about 0.5 (see [1]).

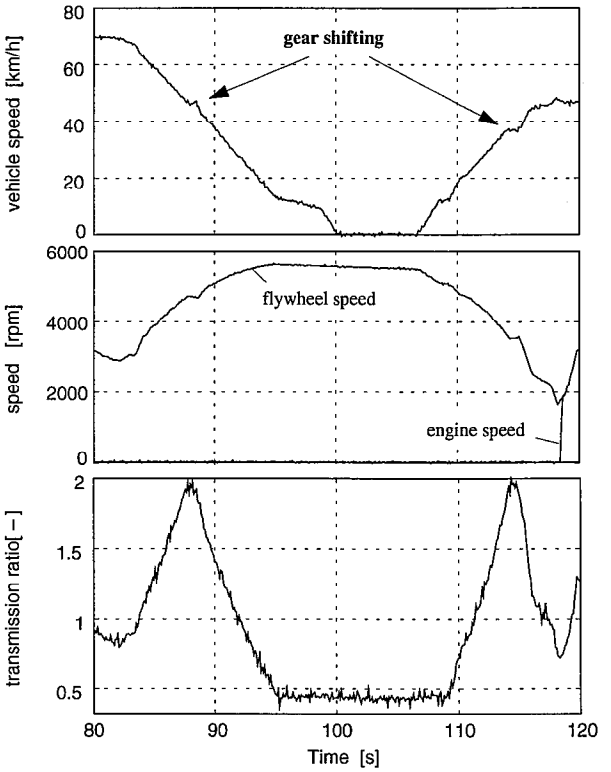

Figure 7: The effect of the gear shifts on the drivability of the Hybrid III vehicle

3.4 Control of the CVT's Gear Ratio

The control input for changing the transmission ratio is the actuator input voltage U_S. This signal corresponds to the relative rate of change of the transmission ratio $(i)^{\cdot}/i$ which is bounded due to the limited power of the CVT hydraulic system (i.e., saturation).

Based on the linearization of the nonlinear CVT model introduced in [11], a PI controller with anti-windup is designed and tested on a dynamic test bench. For the design of the controller parameters, the H_∞-optimization technique is used.

Figure 8 shows a representative frequency response of the control system at the synchronizing transmission ratio $i_S = 1.93$. When the transmission ratio, the input speed of the CVT, and the load torque are increased, the bandwidth (15 rad/s) increases slightly.

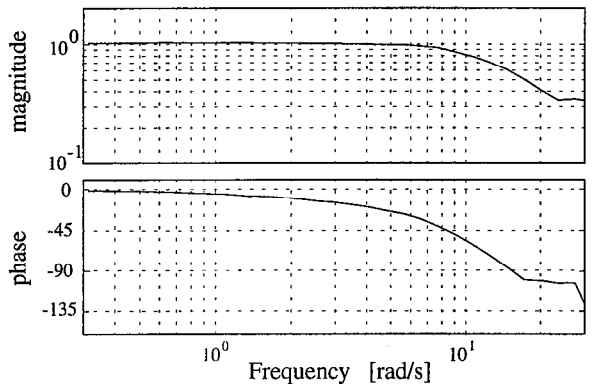

Figure 8: Frequency response for the CVT's gear ratio control system at $i_S = 1.93$

Figure 9 depicts the step responses of the control system and of the corresponding control signal U_S for the low gear.

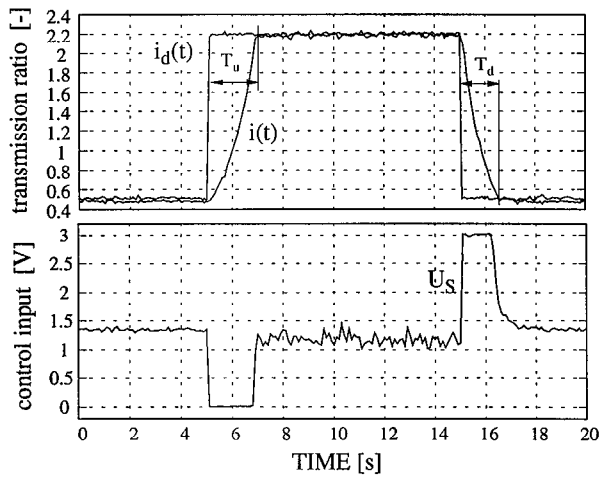

Figure 9: Step response for the CVT's gear ratio control system (low gear, 2400 rpm, 0 Nm)

Clearly, the settling time T_u for changing the transmission ratio from $i = 0.42$ to $i = 2.35$ is larger than the settling time T_d for the opposite direction. This difference is due mainly to a spring installed in the CVT for automatic resets of the transmission ratio to $i = 0.42$. As the transmission ratio is increased, the hydraulic power has to work against the spring force, whereas in the reverse direction the spring force assists in the reset of the transmission ratio.

Another fact evident in Figure 9 is that the controller is not designed conservatively because it uses the full power for a full range change of the transmission ratio.

The maximum relative rate of change of the transmission ratio $(i)^{\cdot}/i$ and, as a consequence, both of the characterizing settling times (T_u and T_d) depend on the input speed of the CVT. This dependency (shown in Figure 10) is found by evaluating the step responses for different input speeds of the CVT in the range from 1800 rpm to 3600 rpm and three different load torques (20 Nm, 60 Nm, and 100 Nm).

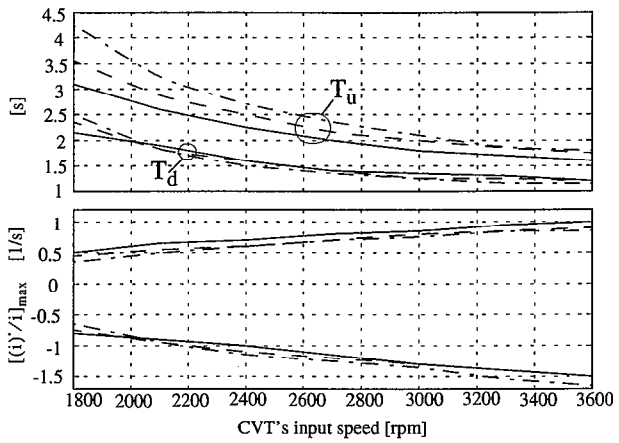

Figure 10: Dependency of T_u, T_d, and $[(i)^{\cdot}/i]_{max}$ on the input speed of the CVT and the load torque

3.5 Control of the Gasoline Engine

In all three operating modes (duty cycle, highway, and throttling mode) the air-to-fuel ratio of the gasoline engine is controlled as depicted in Figure 11.

The feedforward controller calculates the respective air mass in the cylinder for any engine cycle $\hat{m}_{ac}$ based on the displacement volume V_d, the manifold pressure p_m, and the manifold temperature T_m. Using the characterizing parameter for the injection valve m_V and the stoichiometric factor $f_{st} \cong 14.8$, we obtain the nominal injection time t_0 for a stoichiometric air-to-fuel ratio. This value is then corrected by an experimentally determined value in function of the operating point, which is characterized by the engine speed and manifold pressure.

The original lookup tables of the VW Digifant engine management are used for the correction factor necessary to account for the engine temperature and battery voltage.

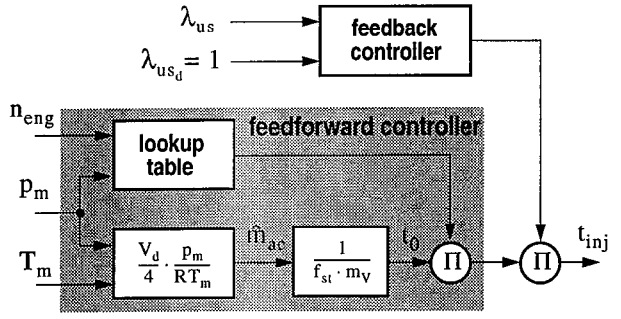

Figure 11: Scheme of the air-to-fuel ratio controller

The feedback controller implemented is a simple PI algorithm with anti-windup. Figure 12 shows the results of measurements made during a single cycle in the duty cycle mode. At 5 s, the flywheel speed reaches the designated lower limit of 1800 rpm. Consequently, the engine starts and reloads the flywheel completely within 10 s. The throttle, which was fully open all the time, is closed during runout. This prevents air from reaching the catalyst. Otherwise, air in the catalyst would cool it off and saturate it with oxygen.

The transients of the air-to-fuel ratios upstream and downstream of the catalyst demonstrate the ability of the controller to achieve a stoichiometric air-to-fuel ratio. When the engine stands still (i.e., before 5 s and after 15.7 s), the value of the air-to-fuel ratio is irrelevant since no air flows.

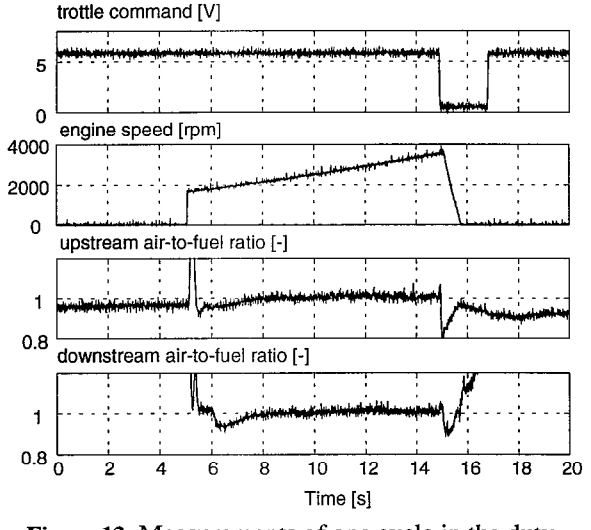

Figure 12: Measurements of one cycle in the duty cycle mode

The VLSI-chip ICX, described in [17], is used for interfacing the actuators for the fuel injection and spark ignition to the process computer. The process computer in this project is the transputer system described in [15].

3.6 Control of the Traction Torque

The Interpretation of the driver's intentions (via accelerator and recuperation pedal) as a desired traction torque leads to the problem of controlling the traction torque. It has been theoretically investigated in detail in [3], [9], and [13]. Some experimental results have been published in [2]. Here we introduce the control laws implemented and focus on the drivability problem of the Hybrid III vehicle by means of experimental results.

In order to design the control laws, the drive line is considered to be rigid. The corresponding mechanical model is shown in Figure 13.

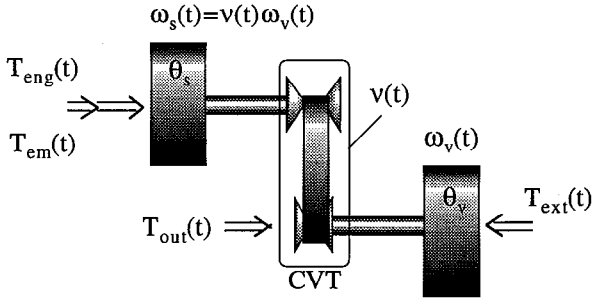

Figure 13: Mechanical model of the rigid drive line.

The torque T_{eng} is delivered by the gasoline engine, T_{em} is the torque produced by the electric motor/generator, T_{out} is the traction torque, and T_{ext} is the external load torque of the vehicle due to aerodynamic drag, roll resistance, and climb angle. The inertia denoted by θ_s represents the inertia of the flywheel whenever the latter is connected to the driveline, while θ_v represents the inertia of the vehicle.

This mechanical model is described by the following equations (see [3]):

$$\dot{\omega}_v = \frac{1}{\nu^2\Theta} \cdot [\nu T_{eng} + \nu T_{em} - \theta_s \omega_v \dot{\nu}\nu - T_{ext}], \quad (1)$$

$$\Theta = \theta_s + \frac{\theta_v}{\nu^2}, \quad (2)$$

and

$$T_{out} = C + D \cdot \dot{\nu}, \quad (3)$$

where

$$C = \left[\frac{\theta_v}{\nu\Theta}(T_{eng} + T_{em}) + \frac{\theta_s}{\Theta}T_{ext}\right] \quad (4)$$

and

$$D = -\left[\frac{\theta_s \theta_v \omega_v}{\nu\Theta}\right]. \quad (5)$$

The hierarchical scheme of the control system is shown in Figure 14. At the top level, the desired traction torque $T_{out_d}(t)$ is translated into a desired rate of change of the total transmission ratio $\dot{\nu}_d(t)$. Integration of this quantity yields the desired total transmission ratio $\nu_d(t)$, which is then used as reference signal for the CVT's gear ratio control system introduced in section 3.4 above.

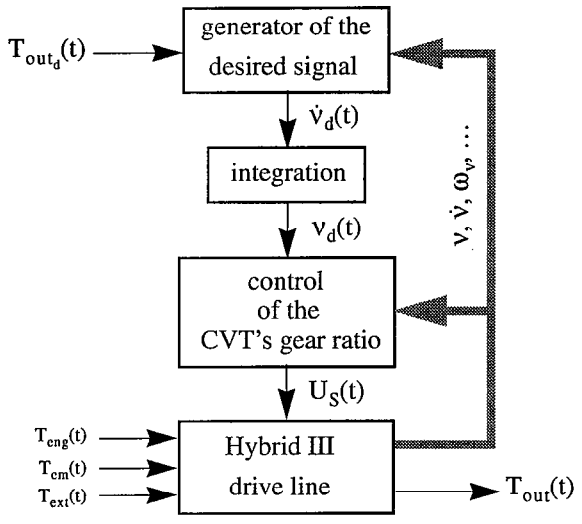

Figure 14: Hierarchical scheme of traction control

The generation of the desired signal $\dot{\nu}_d(t)$ (i.e., the rate of change of the total transmission ratio) depends on the operating mode selected by the strategy master:

Duty cycle mode. In this mode the following control law is implemented (see [2] and [3]):

$$\dot{\nu}_d(t) = \frac{[\hat{C} - T_{out,d}]}{\hat{D}} + K_P \cdot (T_{out,d} - \hat{T}_{out}), \qquad (6)$$

where the first term is the feedforward part determined by direct evaluation of (3), while the second term is the feedback part corresponding to a simple proportional control action. The traction torque in (6) is estimated by:

$$\hat{T}_{out} = T_{ext} + \theta_v \dot{\omega}_v. \qquad (7)$$

The experimental results shown in Figure 15 confirm the tracking performance investigated in [3] by simulation. It can be recognized that start and stop of the engine do not have any noticeable impact on the tracking performance.

Highway mode. Since in this mode the engine is permanently running, the traction torque desired is achieved by the following transmission ratio:

$$\tilde{\nu}_d(t) = \frac{T_{out}(t)}{\hat{T}_{eng}(t)} \qquad (8)$$

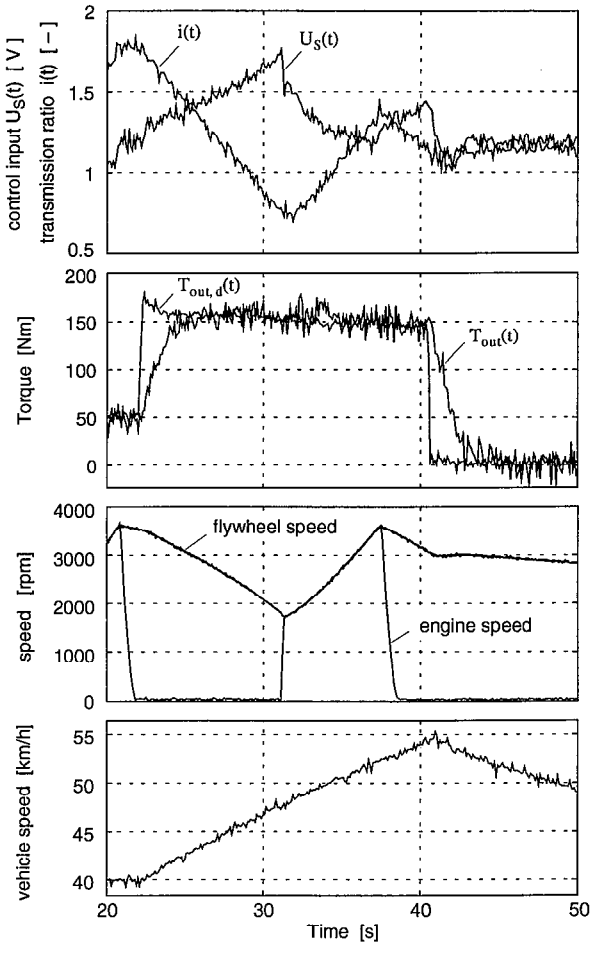

Figure 15: Measurements in duty cycle mode

For smoothing any possible discontinuity by changing the operating modes, as well as for generating the desired rate of change of the transmission ratio $\dot{\nu}_d(t)$, a low pass filter is used (see also [2]):

$$\dot{\nu}_d(t) = \frac{1}{\tau} \cdot [\tilde{\nu}_d(t) - \nu_d(t)]. \qquad (9)$$

Figure 16 shows the experimental results during a change of the operating mode from duty cycle mode into the highway mode. This change occurs at 72.5 s. The control law (9) immediately reverses the direction of the change of the transmission ratio in order to achieve the desired transmission ratio determined by (8). This change of mode causes the mismatch in the traction torque tracking shown in Figure 16.

This drivability problem of the hybrid vehicle has been investigated theoretically in [3]. The experimental results here confirm the theoretical investigations. Referring to the solutions introduced in [3], one can try to reduce the amplitude as well as the duration of the tracking error by using the electric motor and alternative control laws. These improvements are subject of further research.

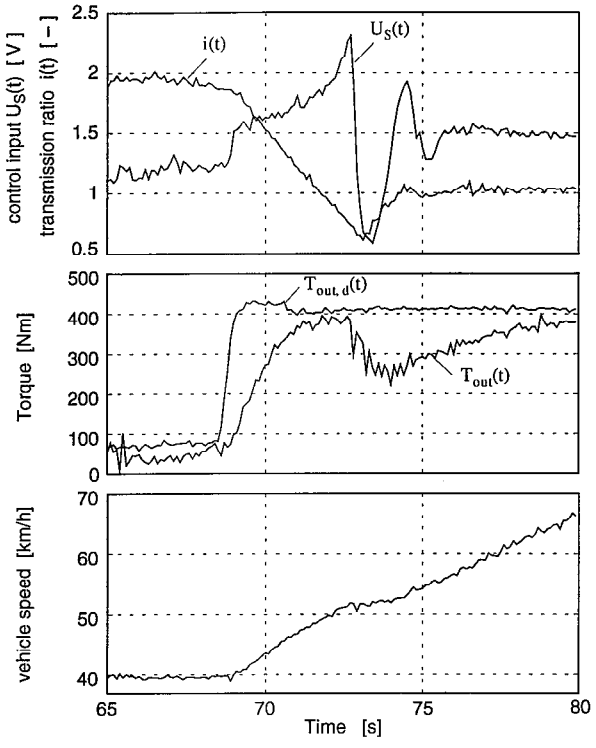

Figure 16: Measurements in highway mode

4 Conclusion

The most important control aspects of the Hybrid III drive line for operating in real road traffic are introduced. The experimental results presented here demonstrate the ability of the simple control laws implemented to make this complex drive line operate as desired. The improvement of the drivability of the Hybrid III vehicle is a subject of further research. It is also planned to replace the air-to-fuel ratio controller by a more sophisticated controller in order to consider the time delay inherent in SI engines.

5 References

[1] Dietrich Ph., Christen U., Wittmer Ch.: *Performance of a Research Hybrid Powertrain Including a Flywheel and a Wide-Range Continuously Variable Transmission*, submit for 6th Int. Congress Lightweight and Small Cars, July 2-4, 1997, Cernobbio.

[2] S. Ginsburg, E. Shafai, Ch. Wittmer, H. P. Geering: *Test Bench Results of a Torque Pedal Interpretation with a CVT-Equipped Power Train*, SAE-Paper 970293, Detroit, 1997, 139–144.

[3] E. Shafai, H. P. Geering: *Control Issues in a Fuel-Optimal Hybrid Car*, Proceedings of the 13th IFAC World Congress, San Fransisco, 1996, 231-236.

[4] M. Ender: *Der Taktbetrieb als teillastverbessernde Massnahme bei Ottomotoren*, Diss. ETH No. 11835, Swiss Federal Institute of Technology (ETH) Zurich, 1996.

[5] M. Ender, H. U. Hörler, Ph. Dietrich: *Duty Cycle Operation as a Possibility to Enhance the Fuel Economy of an SI-Engine at Part Load*, SAE Paper 960229, Detroit, 1996.

[6] Ch. Wittmer: *Entwurf und Optimierung der Fahrstrategien für ein Personenwagen-Antriebskonzept mit Schwungradkomponente und stufenlosem Zweibereichsgetriebe*, Diss. ETH No. 11672, Swiss Federal Institute of Technology, Zurich, 1996.

[7] L. Küng: *Entwicklung einer Drehfeldmaschine mit optimalem Wirkungsgrad für ein Hybridfahrzeug*, Diss. ETH No. 11373, Swiss Federal Institute of Technology, Zurich, 1995.

[8] A. Vezzini: *Optimierung des elektrischen Antriebssystems für ein Hybridfahrzeug*, Diss. ETH No. 11784, Swiss Federal Institute of Technology, Zurich, 1996.

[9] L. Guzzella, A. Schmid: *Control of SI-Engine with CVT's: A Feedback Linearization Approach*, IEEE Transaction on Control Systems, Special Issue on Automotive Control, 1995, 54–60.

[10] A. Schmid, Ph. Dietrich, S. Ginsburg, H. P. Geering: *Controlling a CVT-Equipped Hybrid Car*, SAE Paper 950492, Detroit, 1995, 53–63.

[11] E. Shafai, M. Simons, U. Neff, H. P. Geering: *Model of a Continuously Variable Transmission*, 1st IFAC workshop on Advances in Automotive Control, Monte Verità, Switzerland, 1995, 99–107.

[12] Ch. Wittmer, Ph. Dietrich, L. Guzzella: *Control Strategies for the ETH Hybrid Vehicle*, 1st IFAC workshop on Advances in Automotive Control, Monte Verità, Switzerland, 1995, 126–131.

[13] E. Shafai, A. Schmid, H. P. Geering: *Torque Pedal for a Car with a Continuously Variable Transmission*, SAE Paper 941010, Detroit, 1994, 145–151.

[14] Ph. Dietrich, H. U. Hörler, M. K. Eberle: *The ETH-Hybrid III Car– A concept to minimize consumption and to reduce emissions*, 26th ISATA Conference, Aachen, 1993, 193–200.

[15] H. O. Trutmann: *Control System for Research Car Hybrid III*, WOTUG 15, Aberdeen, 1992.

[16] Hörler, H. U.: *Forschungsprojekt Hybrid III, technisches Konzept eines modernen Hybrid-Oekofahrzeuges*, SAE/SATG-Tagung, Wil, 1991.

[17] H. P. Geering: ICX: *A custom VLSI-chip for engine control*, Int. J. of Vehicle Design, vol. 10, no. 5, 1989, pp. 592–597.